Precise Measurement of H.F. Fields in Models

Institut für Plasmaphysik, Garching

G. Herppich, J. Mantel

IPP 4/51 May 1968

INSTITUT FÜR PLASMAPHYSIK

GARCHING BEI MÜNCHEN

INSTITUT FÜR PLASMAPHYSIK

GARCHING BEI MÜNCHEN

Precise Measurement of H.F. Fields in Models

Institut für Plasmaphysik, Garching

G. Herppich, J. Mantel

IPP 4/51 May 1968

The contents of this report will be presented at the Fifth Symposium on Fusion Technology, Oxford, England 2nd - 5th July 1968.

UDC 621.317.4

Die nachstehende Arbeit wurde im Rahmen des Vertrages zwischen dem Institut für Plasmaphysik GmbH und der Europäischen Atomgemeinschaft über die Zusammenarbeit auf dem Gebiete der Plasmaphysik durchgeführt.

IPP 4/51

Precise Measurement of H.F. Fields in Models

Institut für Plasmaphysik, Garching

G. Herppich, J. Mantel

May 1968

Abstract

To gain performance and stability in plasma heating devices, an exact h.f. field distribution and homogeneity must be determined.

The calculation of the field distribution in complex geometry turned out to be very cumbersome. Measuring methods with high accuracy and stability for sine waves and pulses are demonstrated and analysed.

UDC 621.317.4

INDEX

ABBREVIATIONS

B	Magnetic Inductance
$\overline{B}$	Peak Magnetic Inductance
B_a	Axial Component of Magnetic Inductance
B_r	Radial Component of Magnetic Inductance
C	Capacitance
C_d	A Constant in Cotton-Mouton Rotation Formula
E	Output Signal of a Probe
H	Magnetic Field Strength
$\overline{H}$	Peak Magnetic Field Strength
H_a	Axial Component of Magnetic Field Strength
H_r	Radial Component of Magnetic Field Strength
I_x	Current in x Coils
I_y	Current in y Coils
K	Coil Constants
K_x	x Coil Constant
K_y	y Coil Constant
L	Inductance, Length
Q	Resolution Quality
Q_E	Electrical Resolution Quality
Q_M	Mechanical Resolution Quality
S	Sensitivity
S_o	Maximum Sensitivity
R	Radiation Resistance, Radial Position
U	Voltage
V	Volume, a Constant in Faraday Rotation Formula
X	Linear Position in x Axis Direction
Y	Linear Position in y Axis Direction
a	A Constant
b	A Constant
f	Frequency
n	Number of Lobes in the Directivity Pattern
r	Radius
t	Time
x	Coil Group in x Direction
y	Coil Group in y Direction

Δ	Total Error
α	W.t
β	Arctan $\frac{By}{Bx}$
δ	Skin Depht
δ_2	Second Harmonic
ϵ	Error Component
λ	Wave Length
ϱ	Radius of Curvature
φ	Angle, Rotation Angle
φ_m	Angle of Maximum Sensitivity
φ_p	Position Angle of the Probe
φ_s	Angle of the Field Line
θ	Phase Angle Between Bx and By
ω	$2\pi f$

1 INTRODUCTION

In order to improve performance and stability in plasma heating devices, an exact h.f. field distribution must be determined.

The calculation of field distribution in complex geometry turned out to be very cumbersome. This leads to experimental determination of the field distribution in models.

The accuracy of these measurements must be better than the desired accuracy in reality. This is a major factor in small models, where higher frequencies are used in the model.

One has to decide which parameter should be scaled. Only one of the three, namely skin depth (δ), wavelength (λ), or radiation resistance (R) can be maintained in a non 1 : 1 scale.

$$\delta = a \cdot f^{-\frac{1}{2}}$$

$$\lambda = \frac{c}{f}$$

$$R = b \cdot f^{2}$$

a and b are constants depending on the geometry of the model.

The non-linear effects of the dielectric and magnetic media are usually neglected. Some saturation effects of secondary importance may also take place. This is also true for the frequency variations of the dielectric and magnetic properties of the media.

All these effects tend to deform the true field configuration. One should estimate the introduced error and maintain it, of possible, lower than the desired accuracy.

For sine waves as well as for pulses the over-all error should be less than 0.1 %. In such a measurement facility a 1000 m curvature radius of the field lines must be measurable.

To achieve these requirements the programme described in the following five chapters was started.

2 FIELD MEASUREMENT FACILITIES

A measuring facility proposed by Mantel in an earlier report (1) was built (fig. 1). A stability of smaller than 0.1 % and absolute accuracy smaller than 0,5 % for sine waves and pulses will be achieved after some improvements. The main instabilities occur not in the voltage measuring part, but only in the current generating part.
A. Faraday cage (fig. 7) for models was built and will be expanded to include the mechanical assembly of the probe guidance and control.

3 PROBE DIRECTIVITY DETERMINATION

Magnetic fields are vectors both the magnitude and direction of which have to be determined. In order to evaluate the measurements, the directivity pattern of the probes must be determined.

3.1 Probe Error Theory

Assuming an ideal probe directivity pattern

$$S_{\varphi=\varphi_m} = S_o$$

$$S_{\varphi\neq\varphi_m} = 0$$

the output signal (E) is proportional to $\cos(\varphi_s - \varphi_m)$

φ angle
φ_m angle of maximum sensitivity
φ_s angle of field line
S sensitivity
S_o maximum sensitivity
B magnetic induction

$$\Delta\varphi = \varphi_s - \varphi_m$$
$$E = S \cdot B$$
$$E = S_o B \cos(\varphi_s - \varphi_m) = S_o B \cos\Delta\varphi$$

This gives rise to two errors.

1 - axial error ϵ_a
2 - radial error ϵ_r

The total error Δ depends on the relation of the axial (B_A) and radial (B_R) magnetic inductions.

Usually, $B_A \gg B_R$

$$\Delta = \varepsilon_a + \varepsilon_r \frac{B_r}{B_a}$$

$$\Delta = -(1-\cos\Delta\varphi) + \sin\Delta\varphi \cdot \frac{B_a}{B_r} \qquad (1-\cos\Delta\varphi) \cong \frac{-(\Delta\varphi)^2}{2}$$

$$\Delta \cong -\frac{(\Delta\varphi)^2}{2} + \Delta\varphi \frac{B_r}{B_a} \qquad \sin\Delta\varphi \cong \Delta\varphi$$

For probes which have no ideal directivity pattern an approximation can be used. These probes have several lobes and, in the vicinity of φ_m, a $\cos^n\Delta\varphi$ can be assumed.

$$1-\cos^n\Delta\varphi \cong \frac{n(\Delta\varphi)^2}{2}$$

$$\Delta = -\frac{n}{2}(\Delta\varphi)^2 + (\Delta\varphi)^n \frac{B_r}{B_a} \qquad \sin^n\Delta\varphi \cong (\Delta\varphi)^n$$

This formula is valid for $n = 1$ as well.

3.2 Estimation of Maximum Curvature Radius of Field Lines

The curvature radius is calculated from

$$\varrho = \frac{\left|1+\left(\frac{dy}{dx}\right)^2\right|^{\frac{3}{2}}}{\frac{d^2y}{dx^2}}$$

Let us now deal with specific cases:

Case a) The probe is travelling along a straight line of length L

in $X = 0$ $\quad \frac{dy}{dx} = -\frac{1}{Q_E}$ $\quad Q_E = \frac{B_A}{\text{resolution of } B_R}$

$\frac{dy}{dx}$ on the average is zero. And $\frac{dy^2}{dx^2} = \frac{2}{Q}{L}$

$$\therefore \varrho = \frac{\left|1 + (Q)^2\right|^{\frac{3}{2}}}{\frac{2}{LQ_E}} \qquad \boxed{\therefore \varrho = \frac{LQ_E}{2}}$$

In our case

$L = 0.5$ m

$Q_E = 5000$

$\varrho = 1250$ m.

Case b) The probe is travelling along a field line.

For $X = 0$ $\quad Y = \frac{1}{Q_M}$

For $X = \frac{L}{2}$ $\quad Y = 0$

For $X = L$ $\quad Y = \frac{1}{Q_M}$

$$Q_M = \frac{L}{\text{resolution of Y}}$$

and it can be shown that

$$\boxed{\varrho = \frac{LQ_M}{4}}$$

In our case $L = 0.5$ m

Resolution of $Y = 0.1$ mm

$$Q = \frac{500}{0.1} = 5000 \qquad \varrho = \frac{0.5 \cdot 5000}{4} = 625 \text{ m}$$

One can see that the optimum condition is

$$\boxed{Q_M = 2\,Q_E}$$

Such large radii can only be determined with a very low degree of accuracy, as this is the limit of what is measurable at all. For this reason an unmatching of the Q-factors is not critical as long as the mismatch factor is lower than about five.

3.3 The Probe Directivity Apparatus

Four identical coils were mounted exactly in a cross (fig. 2 and 8) in two groups x and y, according to their positions. A magnetic field of desired strength and direction can be generated at the middle of the cross by varying either the ratio $\frac{B_y}{B_x}$ or the phase angle θ between B_y and B_x.

3.3.1 $\theta = 0 \quad I_x \neq I_y$

When no phase angle exists, the time dependence need not be considered.

$$\frac{B_x}{B_y} = \frac{I_x}{I_y}$$

$$B = K \cdot I$$

$$K_x = K_y$$

$$B_x = K_x \; I_x = K \cdot I_x$$

$$B_y = K_y \cdot I_y = K \, I_y$$

$$B = B_x^2 + B_y^2$$

$$B = k \sqrt{I_x^2 + I_y^2}$$

$$\operatorname{tg} \beta = \frac{B_y}{B_x} = \frac{I_y}{I_x}$$

The position of the probe is characterized by the position angle φ_P

$$\overline{B}\varphi_P = K \sqrt{Ix^2 + Iy^2} \cdot \cos(\varphi_P - \arctan \frac{Iy}{Ix})$$

3.3.2 $I_x = I_y \quad \theta \neq 0$

Alternately, the rotation of the angle can be varied by shifting the phase angle θ between the currents I_x and I_y

$$B_x = K \; I_x \; \sin(wt + \theta)$$

$$B_y = K \; I_y \; \sin(wt)$$

$$\overline{B}\varphi_p = Bx \cos \varphi_p + By \sin \varphi_p$$

$$Bx = B \sin(\alpha+\theta) \qquad \alpha = \omega t$$
$$By = B \sin \alpha$$

$$\frac{\overline{B}\varphi_p}{B} = \cos \varphi_p \cdot \sin(\alpha+\theta) + \sin \varphi_p \cdot \sin \alpha$$

$$2\frac{\overline{B}\varphi_p}{B} = \sin(\alpha+\theta+\varphi_p) + \sin(\alpha+\theta-\varphi_p) + \cos(\alpha-\varphi_p) - \cos(\alpha+\varphi_p)$$

$$\begin{aligned} 2\frac{\overline{B}\varphi_p}{B} &= \sin \alpha \cdot \cos(\theta+\varphi_p) + \cos \alpha \cdot \sin(\theta+\varphi_p) \\ &+ \sin \alpha \cdot \cos(\theta-\varphi_p) + \cos \alpha \cdot \sin(\theta-\varphi_p) \\ &+ \cos \alpha \cdot \cos \varphi_p + \sin \alpha \cdot \sin \varphi_p \\ &- \cos \alpha \cdot \cos \varphi_p + \sin \alpha \cdot \sin \varphi_p \end{aligned}$$

$$\begin{aligned} 2\frac{\overline{B}\varphi_p}{B} &= \sin \alpha \left[2 \sin \varphi_p + \cos(\theta+\varphi_p) + \cos(\theta-\varphi_p) \right] \\ &+ \cos \alpha \left[\sin(\theta+\varphi_p) + \sin(\theta-\varphi_p) \right] \end{aligned}$$

$$2\frac{\overline{B}\varphi_p}{B} = \sin \alpha \left[2 \sin \varphi_p + 2 \cos \theta \cdot \cos \varphi_p \right] + \cos \alpha \left[2 \sin \theta \cdot \cos \varphi_p \right]$$

$$\frac{\overline{B}}{B} = \sin \alpha \left[\sin \varphi_p + \cos \theta \cdot \cos \varphi_p \right] + \cos \alpha \left[\sin \theta \cdot \cos \varphi_p \right]$$

$$\left| \frac{\overline{B}\varphi_p}{B} \right| = \left[\sin^2 \varphi_p + \cos^2 \theta \cdot \cos^2 \varphi_p + 2 \sin \varphi_p \cdot \cos \varphi_p \cdot \cos \theta + \sin^2 \theta \cdot \cos^2 \varphi_p \right]^{\frac{1}{2}}$$

$$\left| \frac{\overline{B}\varphi_p}{B} \right| = (1+2 \sin \varphi_p \cdot \cos \varphi_p \cdot \cos \theta)^{\frac{1}{2}}$$

$$\left| \overline{B}\varphi_p \right| = B \, (1+ \cos \theta \cdot \sin 2 \varphi_p)^{\frac{1}{2}}$$

$$B\varphi_p = \left| \overline{B}\varphi_p \right| \sin(\alpha+\theta_1)$$

$$\tan \theta_1 = \frac{\sin \varphi_p + \cos \theta \cdot \cos \varphi_p}{\sin \theta \cdot \cos \varphi_p}$$

$$B\varphi_p = B \, (1+ \cos \theta \cdot \sin 2 \varphi_p)^{\frac{1}{2}} \cdot \sin \left(\omega t + \arctan \frac{\sin \varphi_p + \cos \theta \cdot \cos \varphi_p}{\sin \theta \cdot \cos \varphi_p} \right)$$

$$\cos(A+B) + \cos(A-B) = 2 \cos A \cdot \cos B$$
$$\sin(A+B) + \sin(A-B) = 2 \sin A \cdot \cos B$$
$$\sin(A+B) + \sin(B-A) = 2 \cos A \cdot \sin B$$
$$\cos(A-B) - \cos(A+B) = 2 \sin A \cdot \sin B$$

3.3.3 $Ix \neq Iy \quad \theta \neq 0$

$$B\varphi_p = Bx \cos \varphi_p + By \sin \varphi_p$$

$$Bx = \overline{Bx} \sin(\alpha+\theta) \qquad \alpha = \omega t$$

$$By = \overline{By} \sin \alpha$$

$$\overline{B} = \overline{Bx} \cos \varphi_p \cdot \sin(\alpha+\theta) + \overline{By} \sin \varphi_p \cdot \sin \alpha$$

$$2B\varphi_p = \overline{Bx} \sin(\alpha+\theta+\varphi_p) + \overline{Bx} \sin(\alpha+\theta-\varphi_p) + \overline{By} \cos(\alpha-\varphi_p) - \overline{By}\cos(\alpha+\varphi_p)$$

$$2B\varphi_p = \overline{Bx} \sin \alpha \cdot \cos(\theta+\varphi_p) + \overline{Bx} \cos \alpha \cdot \sin(\theta+\varphi_p) + \overline{Bx} \sin \alpha \cdot \cos(\theta-\varphi_p) + \overline{Bx} \cos \alpha \cdot \sin(\theta-\varphi_p) + \overline{By} \cos \alpha \cdot \cos \varphi_p + \overline{By} \sin \alpha \cdot \sin \varphi_p - \overline{By} \cos \alpha \cdot \cos \varphi_p + \overline{By} \sin \alpha \cdot \sin \varphi_p$$

$$2B\varphi_p = \sin \alpha \left[2\,\overline{By} \sin \varphi_p + \overline{Bx} \cos(\theta+\varphi_p) + \overline{Bx} \cos(\theta-\varphi_p) \right] + \cos \alpha \left[Bx \sin(\theta+\varphi_p) + \overline{Bx} \sin(\theta-\varphi_p) \right]$$

$$2B\varphi_p = \sin \alpha \left[2\,\overline{By} \sin \varphi_p + 2\,\overline{Bx} \cos \theta \cdot \cos \varphi_p \right] + \cos \alpha \left[2\,\overline{Bx} \sin \theta \cdot \cos \varphi_p \right]$$

$$\left|\overline{B\varphi_p}\right|^2 = \left[\overline{By} \sin \varphi_p + \overline{Bx} \cos \theta \cdot \cos \varphi_p \right]^2 + \left[Bx \sin \theta \cdot \cos \varphi_p \right]^2$$

$$\left|\overline{B\varphi_p}\right|^2 = \overline{By}^2 \sin^2 \varphi_p + 2\,\overline{Bx}\,\overline{By} \cos \theta \cdot \cos \varphi_p \cdot \sin \varphi_p + Bx^2 \cos^2 \varphi_p$$

$$\left|\overline{B\varphi_p}\right|^2 = \overline{By}^2 \sin^2 \varphi_p + \overline{Bx}\,\overline{By} \cos \theta \cdot \sin 2\varphi_p + \overline{Bx}^2 \cos^2 \varphi_p$$

$$\tan \theta_1 = \frac{\overline{By} \sin \varphi_p + \overline{Bx} \cos \theta \cdot \cos \varphi_p}{\overline{Bx} \sin \theta \cdot \cos \varphi_p}$$

$$\tan \beta = \frac{\overline{By}}{\overline{Bx}}$$

$$\tan \theta_1 = \frac{\tan \beta \cdot \sin \varphi_p + \cos \theta \cdot \cos \varphi_p}{\sin \theta \cdot \cos \varphi_p}$$

$$\overline{B\varphi_p} = \left(\overline{By}^2 \sin^2 \varphi_p + \overline{Bx}\,\overline{By} \cos\theta \cdot \sin 2\varphi_p + \overline{Bx}^2 \cos^2 \varphi_p\right)^{\frac{1}{2}} \cdot \sin\left(\omega t + \arctan \frac{\tan\beta \cdot \sin\varphi_p + \cos\theta \cdot \cos\varphi_p}{\sin\theta \cdot \cos\varphi_p}\right)$$

4 PROBE GUIDANCE AND CONTROL

For the precise determination of the field distributions the precise position of the probes must be known. A facility which measures the magnetic field contours (2) and a facility which measures the spatial field with one rotating probe (3) were reported.

In some geometrical configurations it is useful to move the probe on lines which are not straight, but rather complicated. For such lines (e.g. helical and circular lines) a control mechanism for the probe was developed, which allows the probe to be guided on complicated lines.

The probe is mounted on a support which can move in cylindrical coordinates.

Servomotor generators drive the probe while helipots are used to convert the position into an analogue signal. A helical trajectory is achieved when the axial position (x) is proportional to the rotation angle (φ). A spiral trajectory is achieved when the radial position (R) is proportional to the rotation angle (φ).

The control and positioning circuit is shown in fig. 4.

A sketch of the mechanical assembly is shown in fig. 5 - 6.

The mechanical adjustment by optical means is shown in fig. 6.

5 PHYSICAL EFFECTS OF MAGNETIC FIELD PROBES

Magnetic field probes can be divided into several groups according to the physical phenomenon on which they are based:

Reviews on the subject can be found in the literature (4 - 5).

This chapter does not claim to be complete since only those probes which seemed useful were investigated.
It turned out that no probe can satisfy all five of the following conditions:

1) High sensitivity, which is useful for low fields
2) High linearity
3) Good directivity pattern
4) Linear frequency response
5) No lumped components

The probe should be very small in order not to deform the field distribution by its presence.

Some of the methods seem only to work for DC fields, but after modifications they are also applicable to H.F. fields.

5.1 Electromagnetic Probes

Probes which transfer electromagnetic energy into voltage may be regarded as electromagnetic probes. They are divided into:

5.1.1 Coil Probes

Coil probes consist of very small coils which might have more than 100 turns in a volume of less than 1 cubic millimeter. These coils are the most common probes although they present several difficulties.

Thiele and Weber (6) have analysed the theory of coil probes in detail. The design of their coils is based on the necessity of neutralizing the distributed capacities in order to eliminate capacity induced voltages. The accuracy of the probes data was estimated by D. Schmidt (7) to be about 10 %.

Strepa (8) estimates the accuracy which can be achieved to be 1 % when measuring axial fields of $0.1 O_e$ with a 40 mm^3 coil probe.

In an inhomogeneous field in which field derivations of the order $N > 2$ cannot be neglected, the measurement must include several probes (4). Measurements with differential probes and amplifiers (9, 10) and with phase sensitive rectifiers (11) have been reported. Hartz reports an accuracy of about 0.1 % of the axial field strength at a fixed frequency.

5.1.2 Hall Generators

Hall generators are used in measuring alternating magnetic fields because of their high sensitivity and extremely small dimensions. Probes of 10^{-5} mm^3 are reported (12). Probes of similar dimensions achieved an accuracy of 1 % in a magnetic field of 0.01 O_e (13). The long-time stability of temperature compensated probes was reported to be less than 0.003 % (14).

5.2 Mechanical Effects

The influence of magnetic fields on matter gives rise to mechanical forces which can be used for measuring the field strength.

5.2.1 Magnetostriction

The magnetostrictive effects can be used to convert magnetic field strength H into volume change. Also sensitivities of $3 \times 10^{-8} \frac{m}{m \cdot O_e}$ in 30 % F_e-Ni were measured Linearity is good only for strong fields (15). In cobalt, for example, the expansion factor is $6 \times 10^{-10} \frac{m}{m\ O_e}$ and the saturation expansion is 2.6×10^{-5} $\frac{m}{m}$.

5.2.2 Electron Beams

The deflection of electron beams in magnetic fields was used to measure the magnetic fields (16). Is this method the mean field trough which the beam passes is measured and this means that cumbersome evaluation of the measured data has to be accepted. The beam spot on the target limits the spatial resolution and accuracy of the system. The DC beam spot broadens to a line on the target in the HF field. Due to this and the complexity is its application limited to a few cases.

5.3 Thermal Effects

These effects arise when an electronic conductor is exposed to transverse magnetic field and temperature gradients. We distinguish here between the magnetothermal effects and the magnetocaloric effects (17).

5.3.1 Magnetothermal Effects

The phenomena which is observed when a conductor is exposed to the stationary magnetic transverse field and transverse temperature gradient are of a thermomagnetic and galvanomagnetic nature.

5.3.1.1 Thermomagnetic Transverse Effects

If a temperature differenceis maintained across an electronic conductor, a transverse temperature gradient is produced which includes two components (18). The first component is not dependent on the current in the conductor and is refered to as the Righi-Laduc effect, while the other is proportional to the current density and is referred to as the Ettinghausen effect (17, 19). No application of the thermal methods have yet been reported.

5.3.1.2 The Galvanomagnetic Effect

The voltage occurring allong an electronic conductor in a transverse magnetic field with transverse temperature gradient is the galvanomagnetic effect known as the first Ettinghausen-Nernst effect (19).

5.3.1.3 Magnetothermoelectric Effect

The change of thermoelectric effects in magnetic fields is known as the magnetothermoelectric effect. (2).

5.3.2 Magnetocaloric Effect

Thermal effects due to forced change of spontaneous magnetization are called magnetocaloric effects, which include adiabatic cooling or heating of the samples.

5.4 Parameter Change

Electrical and electronic components change their value in the presence of a magnetic field. Although changes of many parameters can be used to measure magnetic fields, only two changes of parameter due to magnetic field seem useful.

The inductance change of a non-air core coil and magneto-resistance (e.g. of bismuth) can be used to measure magnetic field strength. Due to the non-linearities and low sensitivity, it is not recommended for precise and sensitive measurements.

5.5 Optical Activity

The optical activity or the rotation of polarized light in magnetic fields is used in measuring magnetic fields.

5.5.1 The Faraday Effect

The rotation of the plane of polarization produced when plane polarized light passes through certain substances in a magnetic field (the light travelling in a direction parallel to the magnetic field) is called Faraday rotation and is proportional to the field strength. At a measured field strength of 180 kO_e (with a 1.25 cm glass polarizer) the polarization was observed to shift 0.1°. This is equivalent to about 100 O_e or 0.055 % and can be taken as the maximum achieved sensitivity (22).
This effect was reported (23) to be applicable up to magnetic fields of several megagauss (24).

5.5.1.1 The Magnetic Kerr Effect

The second Faraday effect or the magnetic Kerr effect is the rotation of the polarization plane of polarized light when reflected from a mirror exposed to magnetic fields.

5.5.2 The Cotton-Mouton Effect

The rotation of the plane of polarization produced when plane polarized light passes through certain substances in a transverse magnetic field is called Cotton-Mouton rotation and is proportional to the square of the magnetic field strength. The Cotton-Mouton effect is several orders of magnitude less sensitive than the Faraday effect. For 10 kG, for example, the Faraday rotation is about 10^3 higher than the Cotton-Mouton rotation. (25).

Mantel proposed several years ago (26) to use a combination of the Faraday and Cotton-Mouton effects for measuring precise h.f. axial and radial fields.

Let (φ) be the angle of rotation due to a axial field (H_a) and radial field (H_r) according to Faraday rotation (V) and Cotton-Mouton rotation (Cd):

$$\varphi = V \cdot H_a + Cd \cdot H_r^2$$

Let us now assume that in the coils producing the magnetic fields currents I_1 and later I_2, flow which produce magnetic fields H_{a1}, H_{r2}, H_{r2}

$$\varphi_1 = VH_{a_1} + Cd\, H_{r_1}^2$$

$$\varphi_2 = VH_{a_2} + Cd\, H_{r_2}^2$$

$$P = \frac{H_r}{H_a}$$

$$H_r = P \cdot H_a$$

$$\varphi_1 = VH_{a_1} + (Cd\, P^2)\, H_{a_1}^2$$

$$\varphi_2 = VH_{a_2} + (Cd\, P^2)\, H_{a_2}^2$$

$$H_{a_1} = H_1$$

$$H_{a_2} = H_2$$

$$T = Cd \cdot P^2$$

$$\varphi_1 = VH_1 + TH_1^2$$

$$\varphi_2 = VH_2 + TH_2^2$$

$$\left(\frac{H_1}{H_2}\right)^2 = \frac{\varphi_1 - VH_1}{\varphi_2 - VH_2}$$

$$\varphi_1 - \varphi_2 \left(\frac{H_1}{H_2}\right)^2 = V\left[H_1 - \left(\frac{H_1}{H_2}\right)^2 H_2\right]$$

$$\frac{H_1}{H_2} = \frac{I_1}{I_2} = D$$

$$\Phi_1 - \Phi_2 D^2 = V\left[H_1 - DH_1\right]$$

$$H_{a_1} = H_1 = \frac{\Phi_1 - D^2\Phi_2}{V\ (1-D)}$$

$$H_{a_2} = H_2 = \frac{\Phi_1 - D^2\Phi_2}{DV\ (1-D)}$$

$$T = \frac{\Phi_1 - VH_1}{H_1^2}$$

$$T = \frac{\Phi_1 - \dfrac{\Phi_1 - D^2\Phi_2}{D\ (1-D)}}{\left[\dfrac{\Phi_1 - D^2\Phi_2}{V\ (1-D)}\right]}$$

$$T = Cd\ P^2$$

$$P = \sqrt{\frac{T}{Cd}}$$

$$H_r = P \cdot H_a$$

$$H_r = \frac{\sqrt{\dfrac{1}{Cd}\left[\Phi_1 - \dfrac{\Phi_1 - D^2\Phi_2}{D\ (1-D)}\right]}}{\dfrac{\Phi_1 - D^2\Phi_2}{V\ (1-D)}}\ H_a$$

Another method of evaluating T can be used when

$$H = \overline{H} \sin \omega t$$

$$\Phi = V \cdot H + TH^2$$

$$\Phi = V\overline{H} \sin \omega t + T\overline{H}^2 \sin^2 \omega t$$

$$\Phi = V\overline{H} \sin \omega t + \frac{1}{2} T\overline{H}^2 - \frac{1}{2} T\overline{H}^2 \cos 2 \omega t$$

measuring the second harmonic δ_2

$$\delta_2 = \frac{\frac{1}{2} T\overline{H}^2}{V\overline{H}}$$

$$\delta_2 = \frac{T\overline{H}}{2V}$$

and asumming

$$\frac{1}{2} T\overline{H}^2 << VH$$

$$\therefore \overline{H} \sim \frac{\overline{\Phi}}{V}$$

it is found that

$$\delta_2 = \frac{T\overline{\Phi}}{2V^2}$$

$$\delta_2 = \frac{Cd\ P^2\ \overline{\Phi}}{2V^2}$$

$$\boxed{P = V\sqrt{\frac{2\ \delta_2}{Cd\ \overline{\Phi}}} = \frac{H_r}{H_a}}$$

By these methods it is possible without geometrical or directivity errors to measure axial and radial fields simultaneously, as long as the sensitivity of the apparatus is sufficient. This can be achieved either in very high magnetic fields (> 100 kG) or with extremely sensitive receivers (0.001° resolution).

Cotton-Mouton effects are measurable in liquids as well as in vapours (27).

5.6 Resonance Effects

Changing the magnetic fields in a medium gives rise to several physical phenomena of a periodic nature or to resonance effects. Several effects were considered and these are described here. Other gyromagnetic effects and resonances, e.g.

a) Barnett and Einstein de Haas effects
b) ferromagnetic resonance and relaxation
c) paramagnetic resonance and relaxation

are described elsewhere. (28).

5.6.1 Nuclear Magnetic Resonance

Nuclear magnetic resonance (NMR) is the strong absorbtion of an electromagnetic field in a material exposed to magnetic fields of certain values. This phenomenon changes the inductance of a coil in which the material is mounted. The change of inductance, or the frequency shift of a marginal oscillator gives a measure of the magnetic field (29). In practice, the magnetic field is found by measuring the beat frequency when the shifted oscillator is mixed with a constant one (30). Improvements of the method (31) and the application of solid media (instead of water and paraffin earlier) (32) were reported.

Although the NMR is primarily a method of measuring DC fields, it can be used for h.f., too, and it has also been used for measuring pulsed fields (33).

Measurements of fields of 10 O_e (34) to 20 k O_e have been reported (35). Instruments for fields of 2 - 4 kG which can be modified for fields of 100 kG with a resolution of 10^{-5} have been available for years (36).

5.6.2 Electronic Resonance

H.F. field have been measured by making use of electron resonance effects (37). This effect allows fields smaller than those measurable by NMR to be measured.

The electron resonance of metal vapours like rubidium (38, 39) and caesium (40) or gases like helium (41) enables h.f. magnetic fields to be measured.

The illumination of such gases and vapours with circularly polarized light produces higher Zeeman levels.

A strong electron resonance occurs when the frequency of the magnetic field equals the frequency difference of two Zeeman levels. This gives rise to light absorbtion which is measurable by optical means. When the h.f. field was modulated with 80 Hz, magnetic fields of 10^{-5} O_e were measured. (42).

5.6.3 Helicon Resonance

When a block of high conducting material is placed in a large magnetic field and two coils, orthogonal to each other and orthogonal to the magnetic field, are wound on the specimen, resonance phenomena are observed. One coil is driven with constant-amplitude, varying frequency, while the voltage induced in the other coil undergoes sharp resonance peaks which correspond to standing wave modes of the helicon wave in the sample.

Fields of 10 - 80 kG were measured with an error of less than 1 % (43), by measuring the frequency of one of the resonance peaks.

5.6.4 Periodic Size Effects (PSE)

In measuring the magnetoresistance of gallium, a periodic size effect was observed. The magnetoresistance of the gallium probe changes periodically when the magnetic field is gradually increased. This enables precise measurements of DC and h.f. fields (45).

The range of fields is up to 100 kG with an error of less than 1 %. The calibration is done by NMR lines of H^1 and Al^{27} markers. This effect is especially suitable for accurate differential measurements of high magnetic fields (46). Other similar effects like the Shubnikov - de Haas effect and de Haas-van Alphen effects (47) which show periodic field dependence, interfer with PSE measurements.

5.7 Acoustical Effects

Interaction between magnetic field and matter gives rise to magnetoacoustical effects. These effects include the various ultrasonic wave attenuation effects in the presence of magnetic fields, e.g.:

Magnetoacoustic oscillation due to geometrical resonances, cyclotron resonance for acoustic waves and the quantum or de Haas - van Alphen type oscillations. (48). These effects are useful in the higher frequency range while in the lower frequency range, special design transducers can measure the magnetic fields.

5.8 Chemical Effect

Exposing photographic films to high power high frequency fields, the contours of the field can be recorded. The power density must exceed 1o $\frac{mw}{cm}2$ (47) and the frequency above 1 G Hz.

5.9. DATA OF H.F. MAGNETIC PROBES

		VOLUME mm^3	ERROR %	H_{min}	H MEASURED	F USEFUL	WERE USED FOR MEASUREMENT IN		REMARKS
							DC	HF	
5.1 ELECTROMAGNETIC PROBES	5.1.1 COIL PROBES	$> 10^{-2}$	0.1	0.1 G		10Hz - 10 MHz			POOR DIRECTIVITY, LOW SENSITVITY, CAPACITIVE EFFECTS
	5.1.2 HALL GENERATORS	$> 10^{-5}$	0.003 - 1	0.01 G		DC - 30kHz	+	+	INDUCTIVE AND CAPACITIVE EFFECTS
5.2 MECHANICAL EFFECTS	5.2.1 MAGNETOSTRICTION				< 20 kG				POOR LINEARITY
	5.2.2 ELECTRON BEAMS						+	+	POOR ACCURACY
5.3 THERMAL EFFECTS	(a) THERMOMAGNETIC EFFECTS								
	(b) GALVANOELECTRIC AND MAGNETO-THERMOELECTRIC EFFECTS								
5.4 PARAMETER CHANGE	(a) INDUCTANCE						+	+	NON LINEAR CHARACTERISTICS, THE FIELD IS DISTORTED
	(b) MAGNETORESISTANCE						+	+	NON LINEAR CHARACTERISTICS
5.5 OPTICAL ACTIVITY	5.5.1 FARADAY EFFECTS		> 0.05	10^2 G	> 100 kG		+	+	POOR SENSITIVITY AND EXCELLENT DIRECTIVITY
	5.5.2 COTTON-MOUTON EFFECT								
5.6 RESONANCE EFFECTS	5.6.1 NUCLEAR MAGNETIC RESONANCE		10^3		10 - $2 \cdot 10^4$ G		+		
	5.6.2 ELECTRONIC RESONANCE			10^{-5} G			+	+	
	5.6.3 HELICON RESONANCE		< 1		10kG - 80 kG		+		
	5.6.4 PERIODIC SIZE EFFECT		< 1		< 100 kG		+	+	FOR LOW TEMPERATURES
5.7 ACOUSTIC EFFECTS	(a) MAGNETOACOUSTIC EFFECTS					> 10 MHz			
	(b) TRANSDUCERS					< 100 kHz			
5.8 CHEMICAL EFFECTS	FILM EXPOSURE		> 10	*		> 1 GHz	−	+	* POWER DENSITY OF $10 \frac{mW}{cm^2}$ REQUIRED

6 Generation of magnetic fields in models

The magnetic field generated in the models must be high enough to enable accurate measurement.

6.1 The magnitude of the magnetic field

The magnitude of the magnetic field parameters are here given for single-turn coils fed by a generator, or by discharging a capacitor.

For generator feeding:

$$H = \frac{I}{r}$$

H = magnetic field strength in (A/M)
I = current in (A)
r = coil radius in (m)

$$B = \mu_o \cdot H$$

$\mu_o = 4\pi \cdot 10^{-7}$
B = magnetic inductance in $(\frac{V \text{ sec}}{m}) = (10^4 \text{ G})$

For capacitor discharge

$$\frac{1}{2} CU^2 = \frac{1}{2} LI^2$$

$$\frac{1}{2} LI^2 = \frac{1}{2} \cdot H \cdot B \cdot V$$

C = capacity (F)
U = voltage (V)
L = inductivity (Hy)
V = volume of the coil (m^3)

$$CU^2 = \mu H^2 V$$

$$H = \sqrt{\frac{c}{\mu_o V}} \cdot U$$

$$B = \sqrt{\frac{c \mu_o}{V}} U$$

Example: A 16 µF capacitor is charged to 100 V and discharged to a 30 cm long coil 2.5 cm in diameter.

$$V = 0.3 \cdot \frac{\pi}{4} \cdot (2.5 \cdot 10^{-2})^2 = 1.47 \cdot 10^{-4}\ m^3$$

$$B = \sqrt{\frac{1.6 \cdot 10^{-5} \cdot 4\pi \cdot 10^{-7}}{1.47 \cdot 10^{-4}}} \cdot 10 = 3.70\ 10^{-3}$$

$$B = 3.7o \cdot 10^{-3}\ \left(\frac{V\ sec}{m^2}\right) = 37\ G$$

6.2 Feeding of models (G. Herppich)

The models here are all fed with h.f. current, unlike other models and potential analogues (50) used for the same purpose.

There are several possibilities of feeding the models which must be taken into account when h.f. fields are measured. The advantage and disadvantage must be compared in order to optimize the measurement facility.

6.2.1 Feeding with CW

The measurement of models with continuous waves is the simplest of all the feeding methods. Any R.F. generator which meets the requirements with respect to power, distortion, and stability can be used. Most of the generators have high output impedance, which calls for matching units, this generally being realized by a transformer.

What makes C.W. attractive is the possibility of using capacitors as constraining elements (for realization of a constrained current distribution in the collector), in order to reach maximum current at series resonance.

The fact that the currents seldom resemble pure sine waves makes it difficult to use field distributions measured with sine waves. The measurement of a broad frequency response seldom solves this problem, since the real current includes a broad continuous spectrum and transients.

In order to overcome this difficulty, pulse generator feeding can be applied.

6.2.2 Feeding with pulse generators

The wave form of the pulse used to stimulate the field distribution must be similar to the original current wave form. For this reason, the matching unit in the C.W. case must usually be replaced by a pulse or broadband power amplifier. Although the passive matching units (e.g. pulse transformers) can achieve good frequency response and low phase distortions, they cannot match two lighty different impedances simultaneously.

In such cases of high input to output impedance ratio, a pulse or power amplifier is recommended.

A power amplifier with the following data was built in the IPP Garching:

Band:	200 Hz - 2 MHz (3 dB)
	1 kHz - 1 MHz (+ 0% - 10%)
Input:	120 - 1200 ohm
	3 V (minimum)
	differential input
Output:	2 x 200 W
	1 - 3 Ω
	2 x 40 A (P. to P.), R < 1 Ω
	2 x 100 v(P. to P.), no load
	distortions 10 %

The high current output is necessary for feeding the model, in order to allow sensitive and accurate measurement in the presence of electrical noise. Due to this and the fact that the current constraining elements consist of resistors which attenuate the current, a screened cage must be used sometimes.

A screened cage in which the models and measurement facility are placed was built in the IPP in Garching (fig. 7)

6.2.3 Capacitor charge feeding

The most common current pulse is the damped oscillation. It is generated by the discharge of a capacitor into a coil. These discharges have higher power than that in conventional pulse generators and amplifiers and also have very low impedances. This feeding method is limited to pulses which can be synthesized from charging, discharging, switching, including crowbar switching.

The use of mercury wetted relays of low impedance and low +) jitter in model simulation was reported (51 - 52).

The limitation of the relays is mainly due to the high jitter ++) (53) and, secondly, to inductances that cannot be neglected. The delay time of relays may generally present difficulties, but these can be neglected as long as spark gaps are simulated.

The transistor switches built in the IPP in Garching and elsewhere (54 - 55) can be used for many purposes, although leakage currents, offset voltages, and insufficient decoupling cannot generally be neglected. Switches for low leakage currents and low offset voltages have been reported (56 - 57). The decoupling problem is to be tackled in the IPP in Garching by introducing the Hewlett Packard photon coupled Isolators.

7 Summary

The state of the art of measuring h.f. magnetic fields has been reviewed. The programme initiated, in the IPP in Garching and the experience therby gained has been described. A bibliography on the subject is given, special attention being paid to probe physics, while mathematical analysis is only used in those cases where it is not available in the literature.

+) compared with conventional relays

++) compared with spark gaps and solid state switches.

8 Bibliography

1 A. Knobloch, J. Mantel, G. Roos, H. Schlageter, F. Werner: "Geometric High Frequency Models and Potential Analogs for the Determination of Current and Field Distributions" IPP 4/30 May 1966, presented at the 4th Symposium on Engineering Problems in Thermonuclear Research Frascati Italy, May 1966

2 Freeman R.: "Measurement of Magnetic Field Contours" J. of Sci. Instr. 38 (1961) 8 pp. 318-321

3 Eulenberg HP.: "Schaltungsprinzip einer Apparatur zur Messung räumlich verteilter Magnetfelder". Int. Elek. Rundschau (1968) I, pp. 9 - 10

4 Hermann P.K.: "Magnetische Messungen" ATM (1964) 10, pp. 237-240

5 Germain, C.: "Nuclear Instruments and Methods 21 (1963) I pp. 17 - 46

6 Thield W. and Weber W.: "Magnetsondenmessungen und die Grenzen ihrer Anwendbarkeit" IHT-Bericht Nr. 2-7. Institut für Hochtemperaturforschung der Universität (Technische Hochschule) Stuttgart - July 1964

7 Schmidt D.: "Sondeneichgerät, elektrische Überprüfung von Spulen und Schleifensonden" Semesterarbeit Inst. f. Hochtemperaturforschung der Universität (Technische Hochschule) Stuttgart 1961

8 Stepa N.I.: "Pribory i Technika Eksperimenta" 6 (1961)

9 Pearson A.: "J. SCI Instrum." 39 (1962) pp. 8 - 10

10 Hartz F.: IPP Report to be published 1968

11 Karassjow W.W.: Westnik Elektropromyslennosti
34 (1963) 3, pp. 57-58

12 Schieffman C.A.: Rev. Sci. Instrum 33 (1962) 2, pp. 2o6-207

13 Roshon Jr.DD.: Rev. Sci. Instrum, 33 (1962) 2, pp. 201-206

14 Zingery W.L.: Rev. Sci. Instrum. 32 (1961) 6, pp. 706-708

15 Am. Inst. of Phys. Handbook 2nd Ed.
Mc. Graw Hill, New York 1963, pp. 5 - 194

16 Murrman H., Schwink Ch.
z. angew. Physik 13 (1961), pp. 189-193

17 Stoner E.C.: "Magnetism and Matter"
Methuen and Co. London 1934

18 Landolt-Börnstein Volume II 9
Springer Verlag Berlin 1962, pp. 1-136

19 see (10) pp. 9 - 34

20 see (18) volume II 6

21 Chikazums S. and Charap S.H.: "Physics of Magnetism"
John Willey N.Y. 1964

22 Alers P.B.: Rev. Sci. Instrum. 33 (1962) 1, pp. 74-75

23 Mccartan J., Barrault M.R.: "An Optical Magnetic Probe"
4th Symposium on Engineering Problems in Thermonuclear Research
Frascati (Roma) Italy 23 - 27.5.1966

24 Herlach. F., Koepfel H. Luppi R. and van Montfoort:
"Faraday Rotation in Megagauss Fields"
Proceeding of the Conference on Megagauss

25 Condon and Odishaw: "Magnetic Field Generation by Explosives and Related Experiments"
Frascati Italy Sep. 21-23 1965, pp. 471 - 482
Handbook of Physics
Mc Graw Hill New York 1958, pp. 6 - 17

26 Mantel J. not published report IPP 1964

27 Novikov L.N.: "The Cotton-Mouton Effect in Optical Oriented vapors of Alkali Metals"
JETP Letters (English translation)
6 (1967) 1, pp. 11-13

28 See (18)

29 Pound R.V., Knight W.D.: "A Radiofrequency Spectograph and Simple Magnetic Field Meter"
Rev. Sci. Instr. 21 (1950) 3, pp. 219-225

3o Rogers R.M., Kantor R.H.: "Frequency Shift Magnetometer"
Rev. Sci. Instr. 32 (1961) 11, pp. 1230-1234

31 Freeman R. and Pound R.V.: "High Resolution NMR Spectrometer with the Radio Frequency Controlled by the Magnetic Field"
Rev. Sci. Instr. 31 (1960) 2, pp. 103-106

32 Rogers S.J.: Sci. Instr. 38 (1961) 7, pp. 308-309

33 Pollak V.L., Slater R.R.: "Input Circuits for Pulsed NMR"
Rev. Sci. Instr. 37 (1966) 3, pp. 268-272

34 Faini G., Svelto O.: "Alta Frequenza"
3o (1961) 5, pp. 796-798

35 Ivanov R.B., Popov A.I., Sorokin P.V.:
"Pribory i Technika Eksper 6 (1961) 3, pp. 167

36 Rev. Sci. Instr. 33 (1962) 6, pp. 702
(Alph-Scientific Lab. Instrument)

37 Spokas E.O. Panos M:
Rev. Sci. Instr. 33 (1962) 6, pp. 613-617

38 Wireless World 67 (1961) 5, pp. 280

39 Parasons L.W., Wiatar Z.M.
J. Sci. Instr. 39 (1962) 6, pp. 292-300

40 Malmar.L., Mosnier J.P.
Ann. Radioelectr. 16 (1961) 63, pp. 3-8

41 Rice J.R.J.A.
LRE. Inter. Conven. Record 9 (1961) 9, pp. 244-248

42 See (28)

43 Houck J.R., Bowers R.: "New Type of Flux Meter for the measurement of High Magnetic Fields at Low Temperatures"
Rev. Sci. Instr. 35 (1964) 9, pp. 117o-1172

44 Munarin J.A., Marcus J.A.:
in Proc. of the Inter. Conf. on Low Temp. Phys.
Columbus Ohio 1964 (Plenum Press Inc. New York 1965)
part B, pp. 743

45 Fonner S., McNiff J.R.E.J.
Bull. Am. Phys. Soc. 10 (1965) pp. 351

46 Fonner S., McNiff I.R.E.J.
"Calibration and Differential Field Measurement of High Magnetic Fields by Means of a Periodic Size Effect in Gallium"

47 See (18) pp. 1-12

48 Bhatia A.B. Ultrasonic Absorption
Clarendon Press Oxford 1967, pp. 306-315

49 Lizuka K.: "Mapping of Electromagnetic Fields by Photochemical Reaction"
Electronics Letters 4 (1968) 4, pp. 68-69

50 Knobloch A., Mantel J., Roos G., Schlageter H., Werner F.: "Geometric High Frequency Models and Potential Analogs for the Determination of Current and Field Distribution"
IPP 4/30 - May 1966

51 Herppich G.: "Program Controlled Switching Set for Switching Circuit Analog Models" (in German)
IPP 4/20 - January 1965

52 Herppich G., Knobloch A.: "An Analog System for the Disign of Switched Discharge Circuits in Plasma Physics"
IPP 4/29 - April 1966

53 Mantel J.: "Definition of Jitter and a Fast Method to Deduce It"
Electronics Letters 2 (1966) 8, pp. 300

54 Bodin H.A.B. Heywood G.C.H.: "Low Voltage Switched Capacitor Bank for Determing Pulsed Magnetic Field Distribution"
CLM - P 134 - April 1967

55 Bodin H.A.B. Heywood G.C.H.: "Low Voltage Transistor-switched Capacitor Bank for Determing Pulsed Magnetic Field Distributions"
J. of Sci.Inst. (1968) 2 Vol. 1 pp. 347-350

56 Bellamy N.W., Styler S.R.: "Analogue Switches for Computer Mode Control"
Electronic Engineering (1967) 8, pp. 512-515

57 Millman J., Taub H.: "Pulse, Digital, and Switching Waveforms" McGraw-Hill, New-York 1965, pp. 627-641

9 The Figures

1 H.F. Magnetic Field Measuring Facility
(Circuit Diagram)

2 Probe Directivity Apparatus - Circuit Diagram

3 Probe Directivity Measuring Circuit

4 Control and Positioning Circuit of Probe Guidance

5 Mechanical Assembly of Probe Guidance Sketch I

6 Mechanical Assembly of Probe Guidance Sketch II

7 The Faraday Cage For Models

8 Mechanical Assembly of the Probe Directivity Apparatus

9 Model of Isar I

10 Model of the Turbulence Heating Experiment

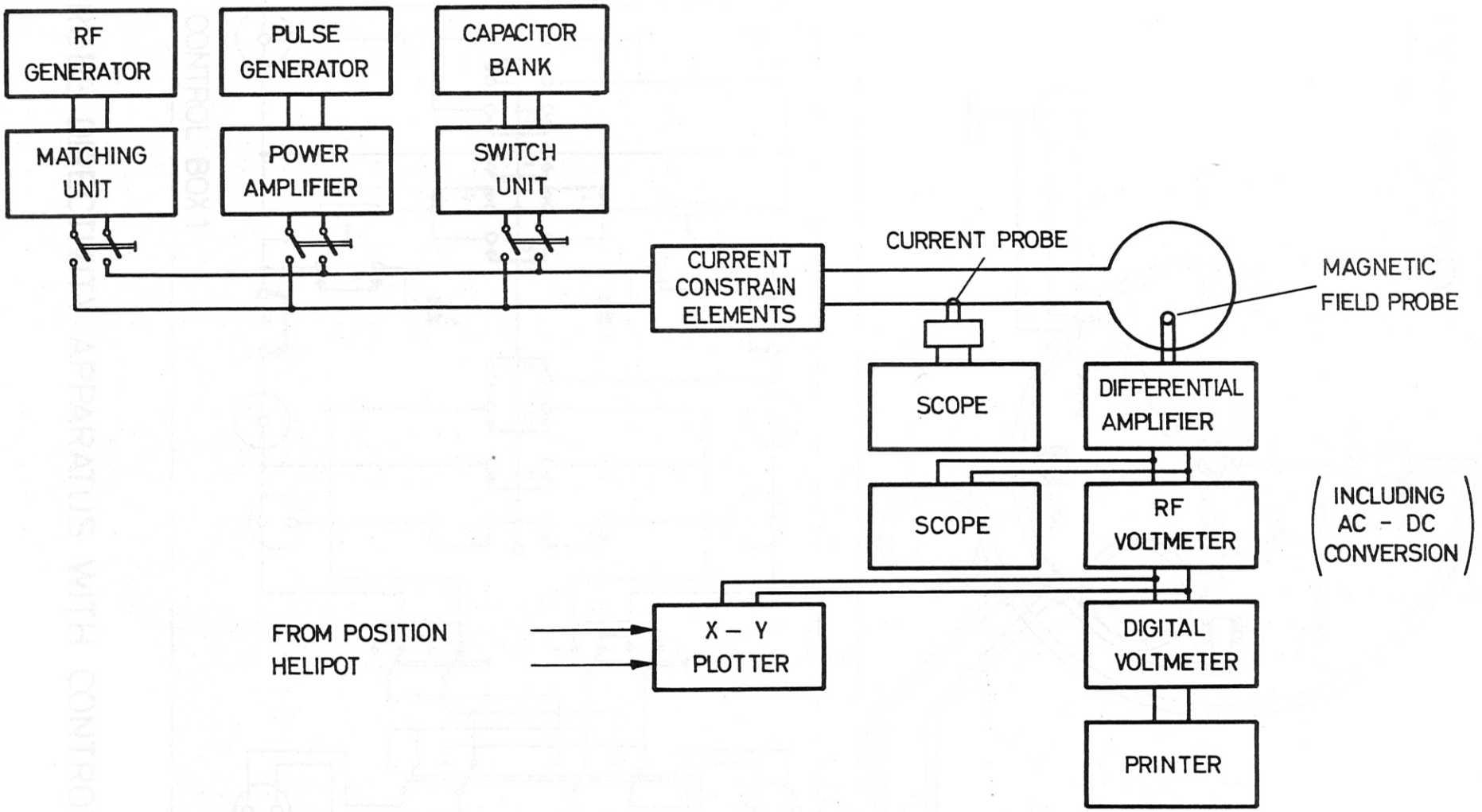

FIG. 1

MAGNETIC FIELD MEASUREMENT FACILITY

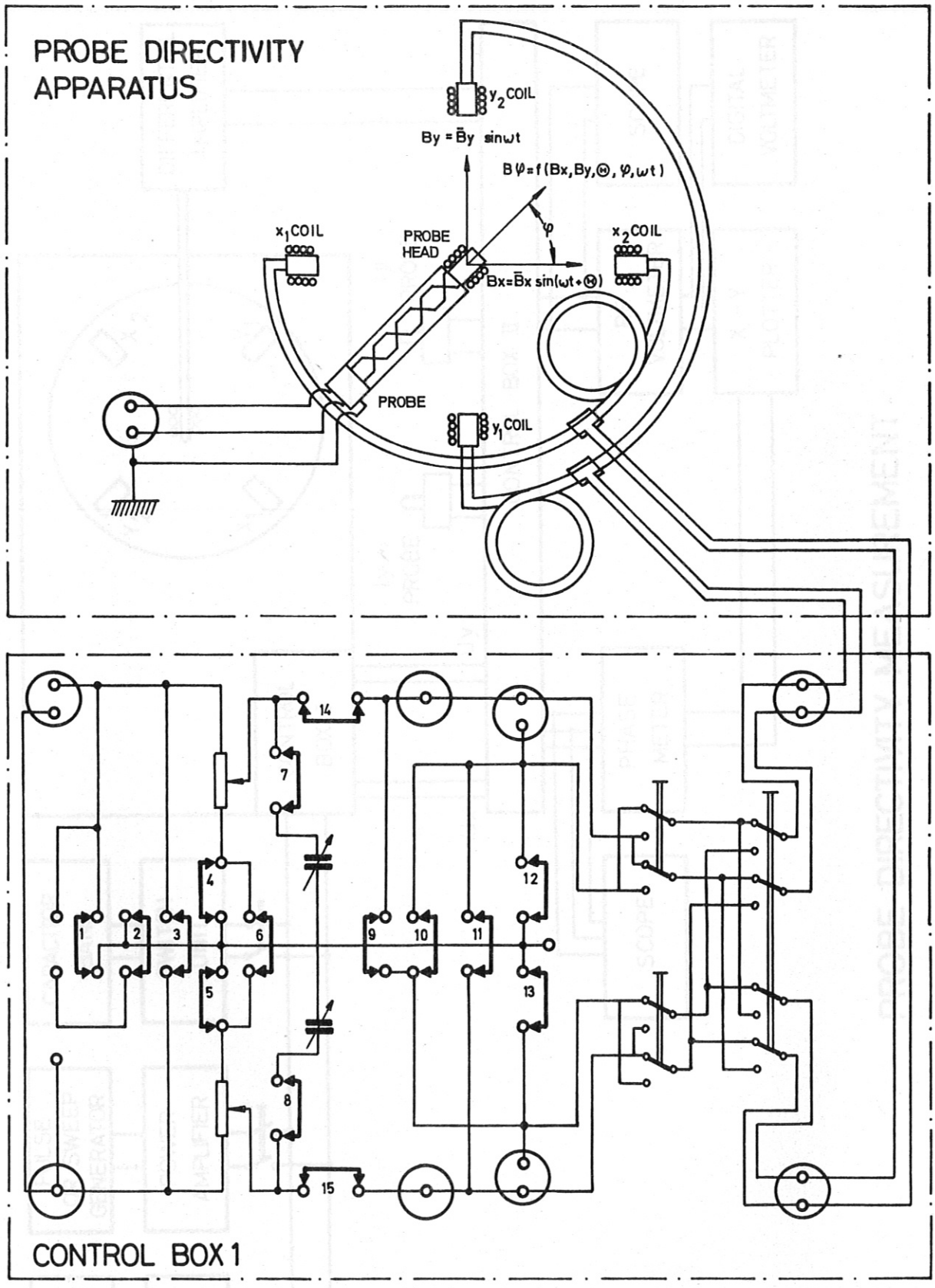

PROBE DIRECTIVITY APPARATUS WITH CONTROL BOX

P4-140

FIG. 2

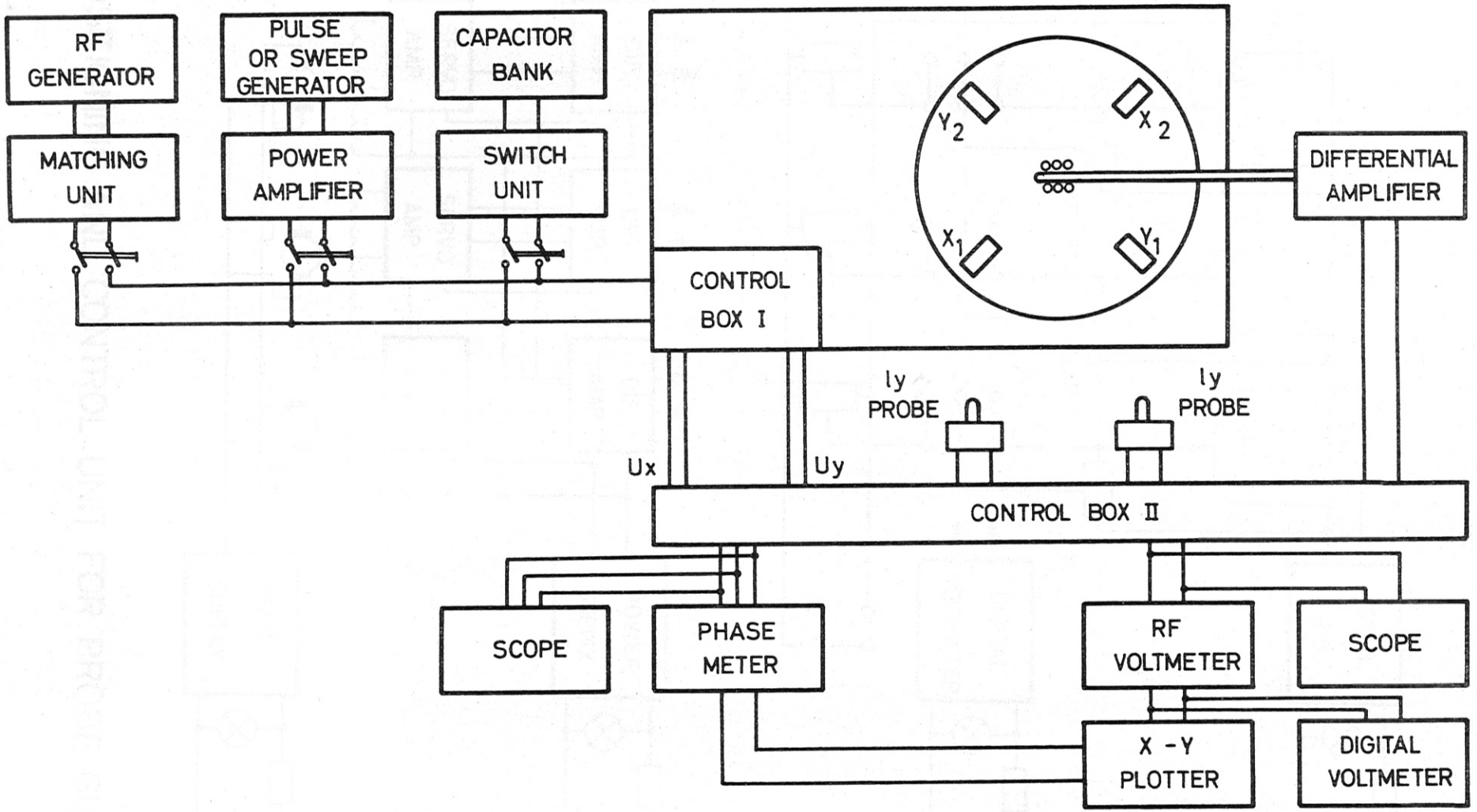

FIG. 3

PROBE DIRECTIVITY MEASUREMENT

P4 - 141

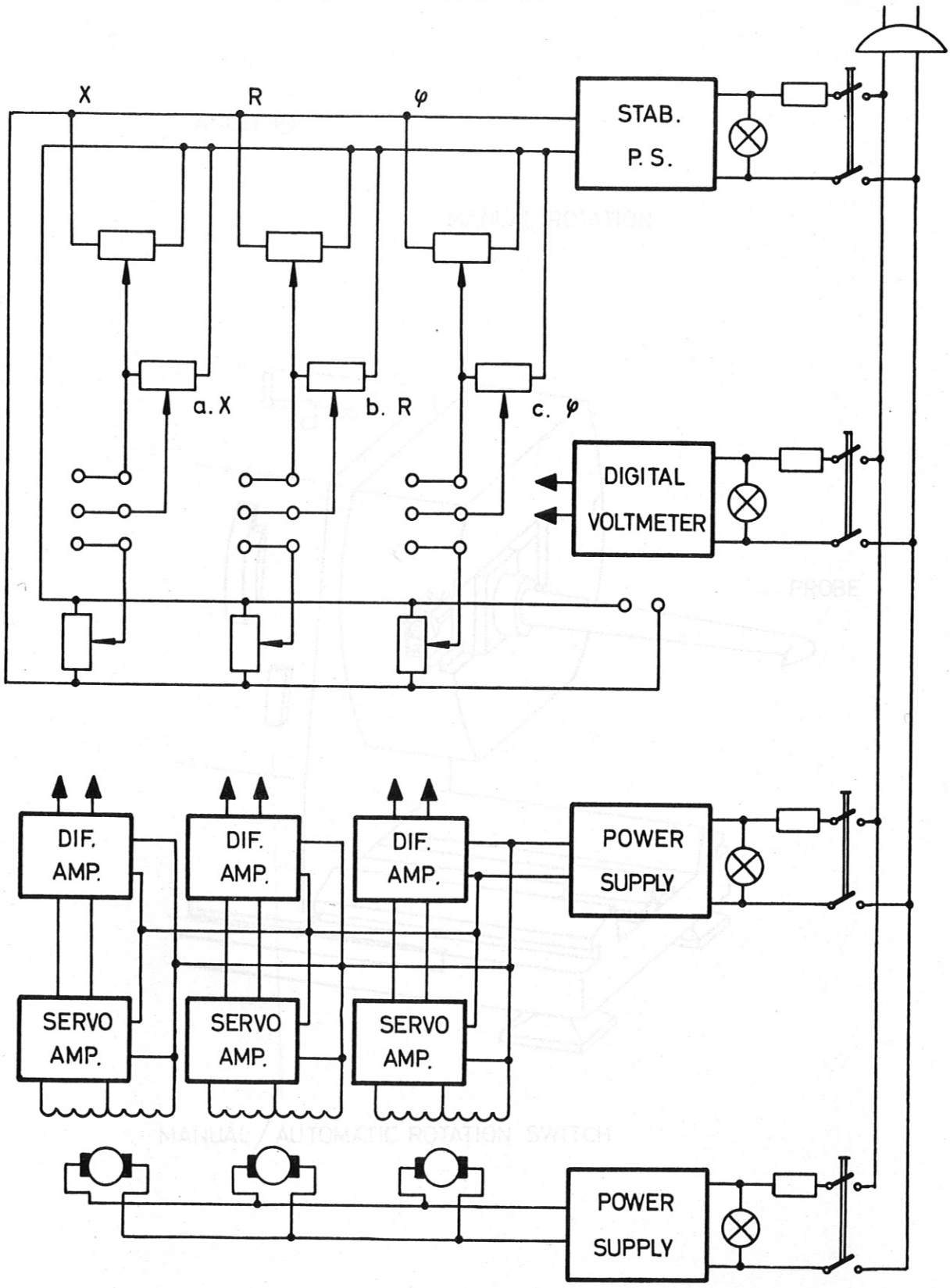

POSITIONING AND CONTROL UNIT FOR PROBE GUIDANCE

P4-142

FIG. 4

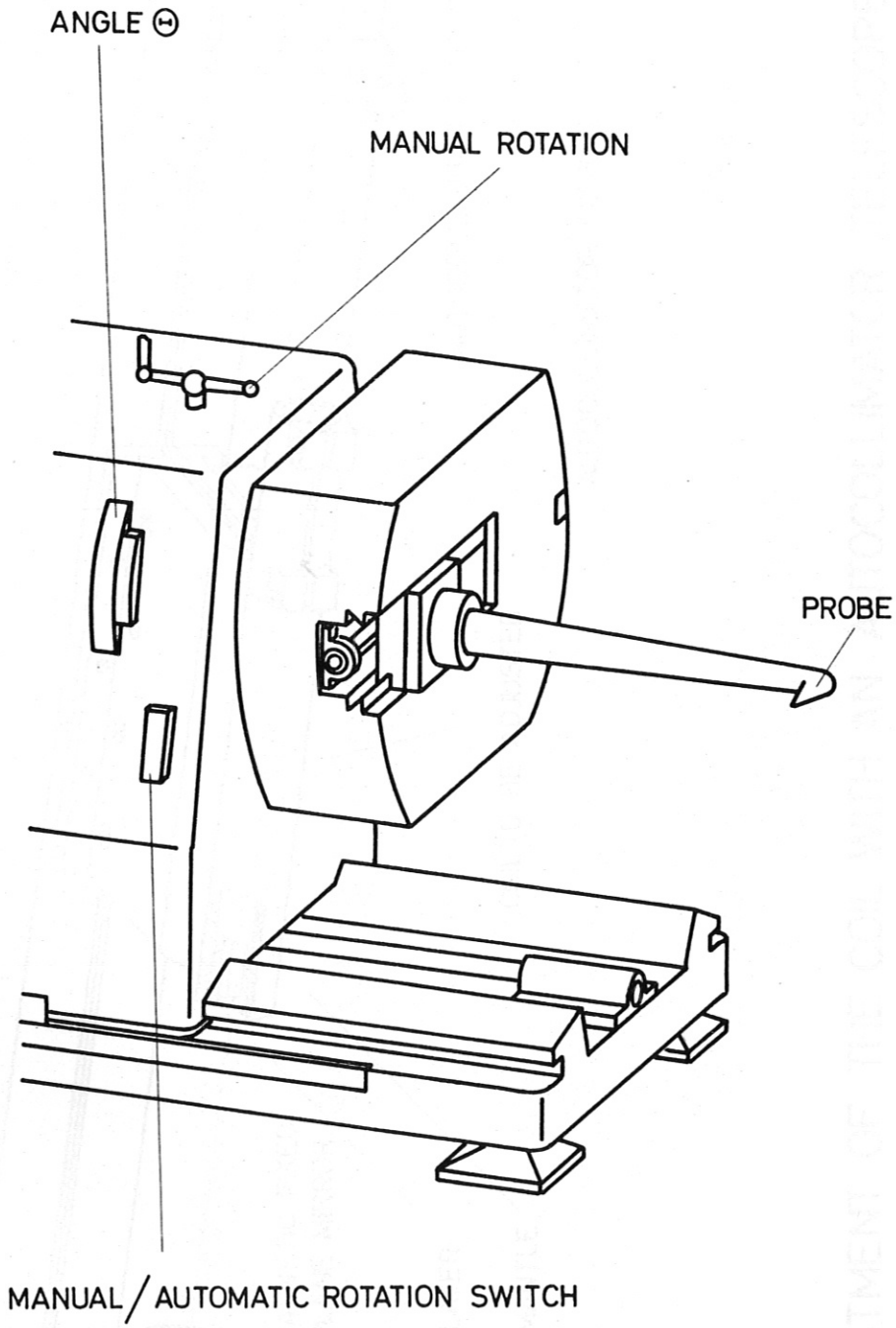

SKETCH OF THE MECHANICAL ASSEMBLY
OF THE PROBE GUIDANCE AND CONTROL

P4-143

FIG. 5

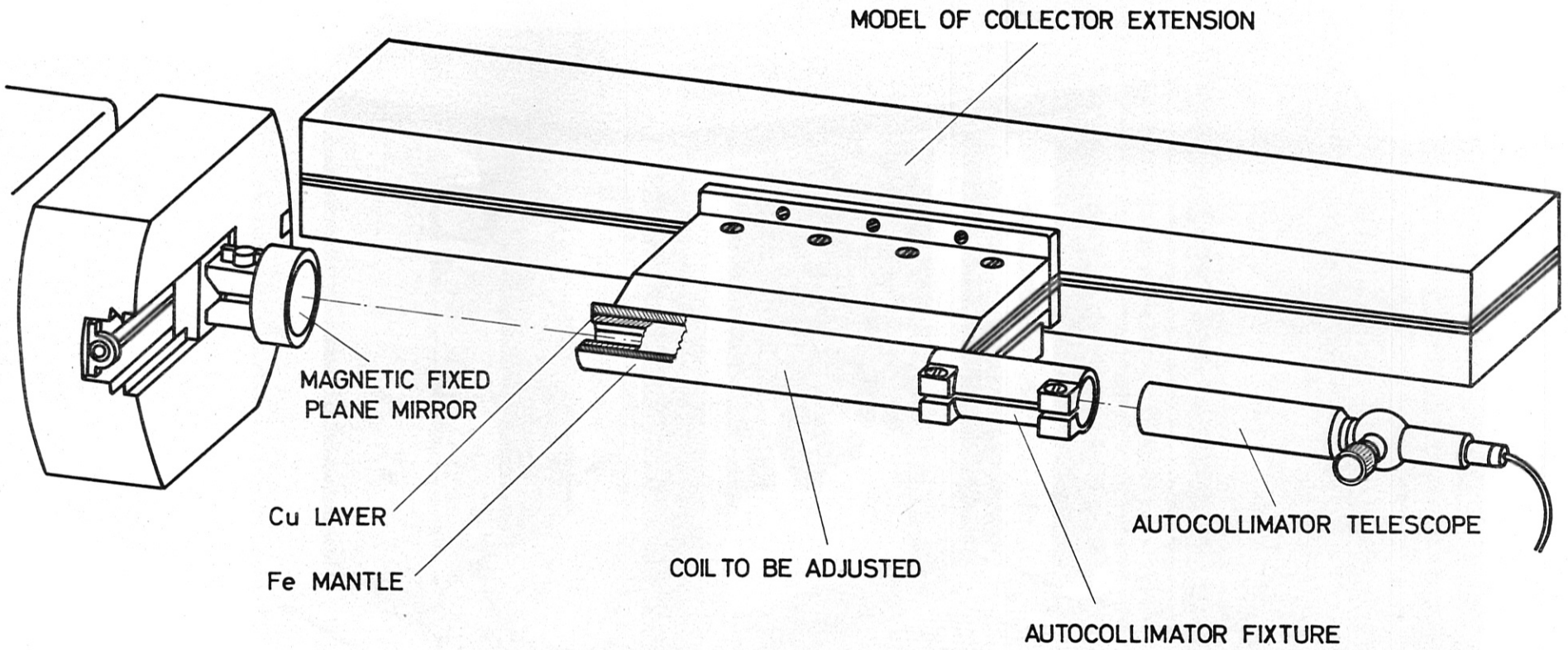

FIG.6

ADJUSTMENT OF THE COIL WITH AN AUTOCOLLIMATOR TELESCOPE

P4-144

SCREENED CAGE FOR MODEL MEASUREMENTS

FIG. 7

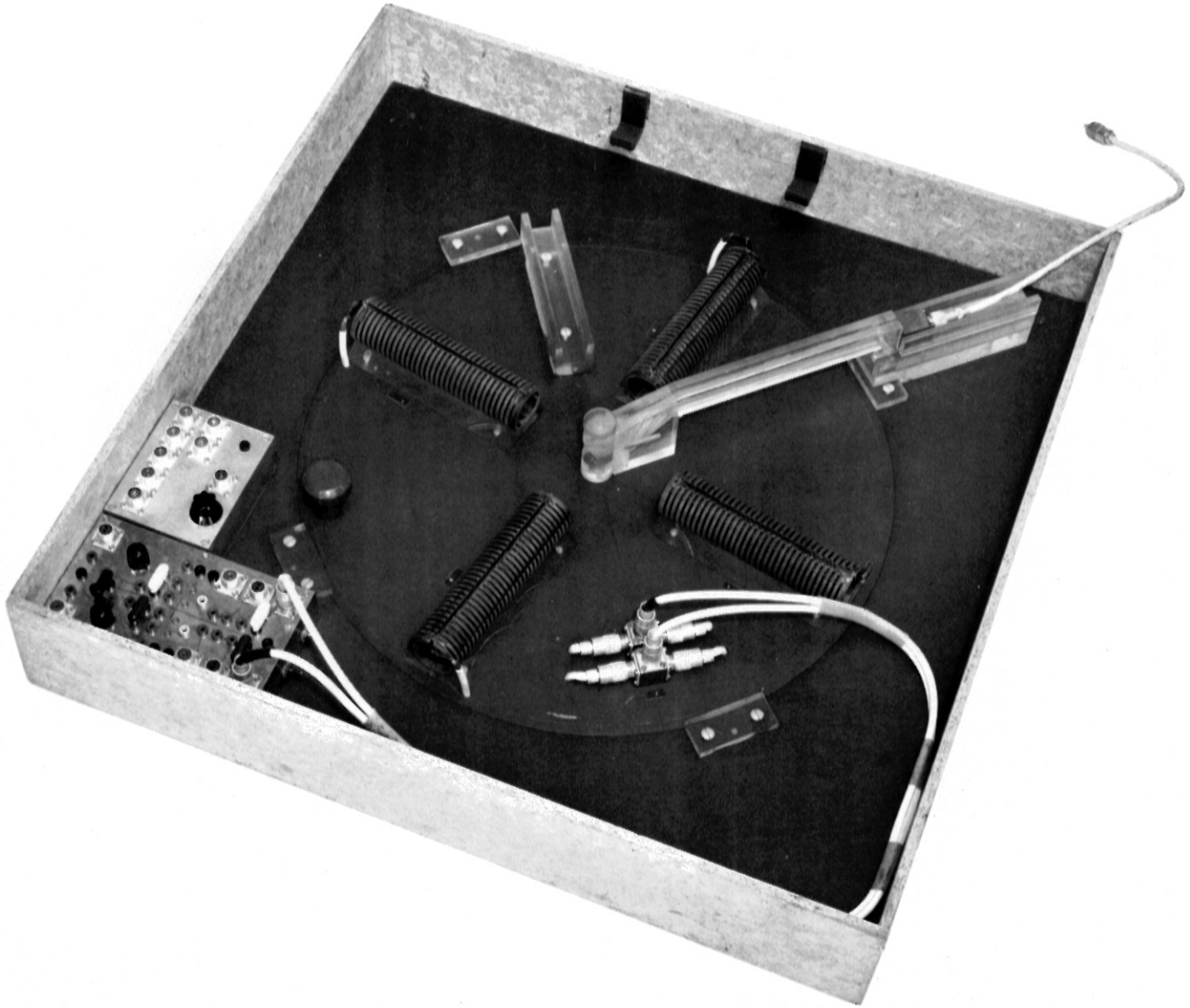

FIG. 8

PROBE DIRECTIVITY APPARATUS WITH CONTROL BOX

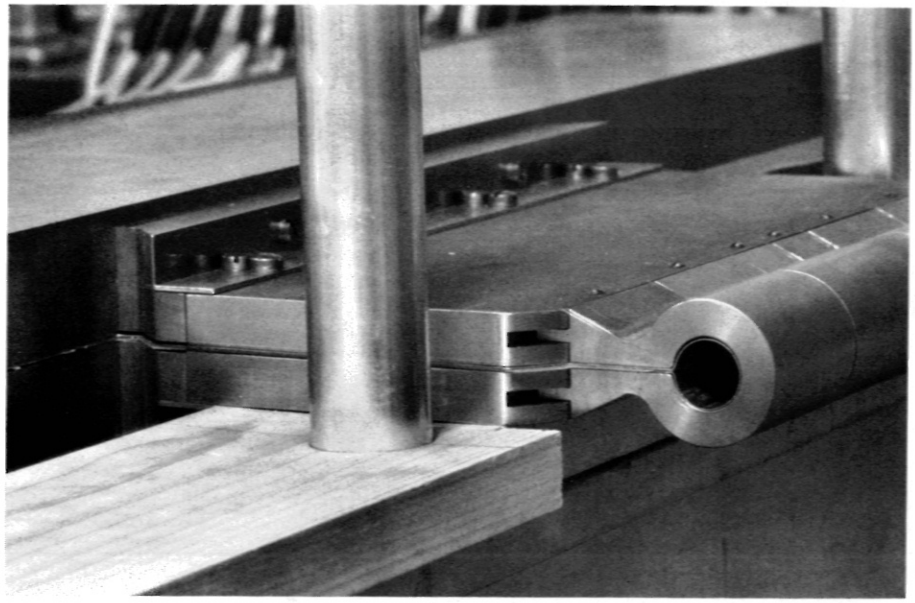

P 030 1,5/2,6 MJ - Theta-Pinch Isar I
Model of collector extension (detail)

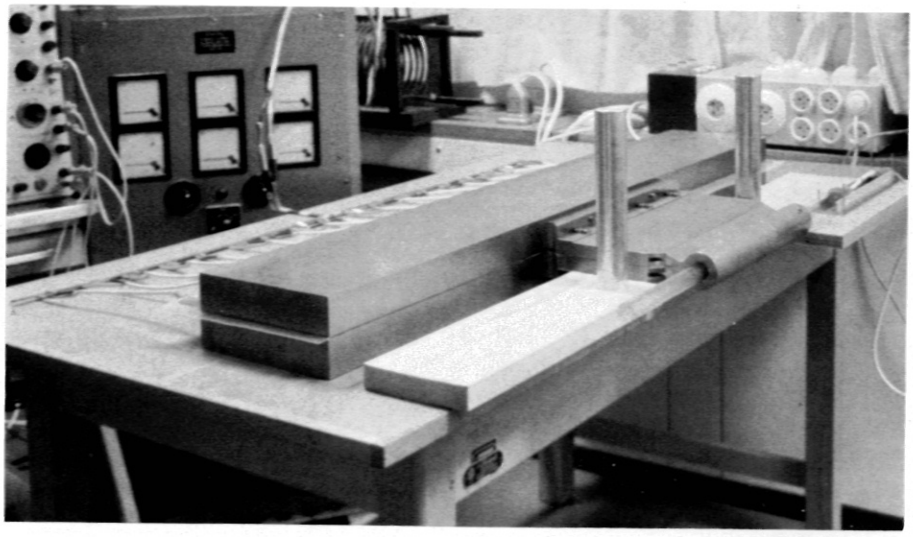

P 031 1,5/2,6 MJ - Theta-Pinch Isar I
Model of collector extension

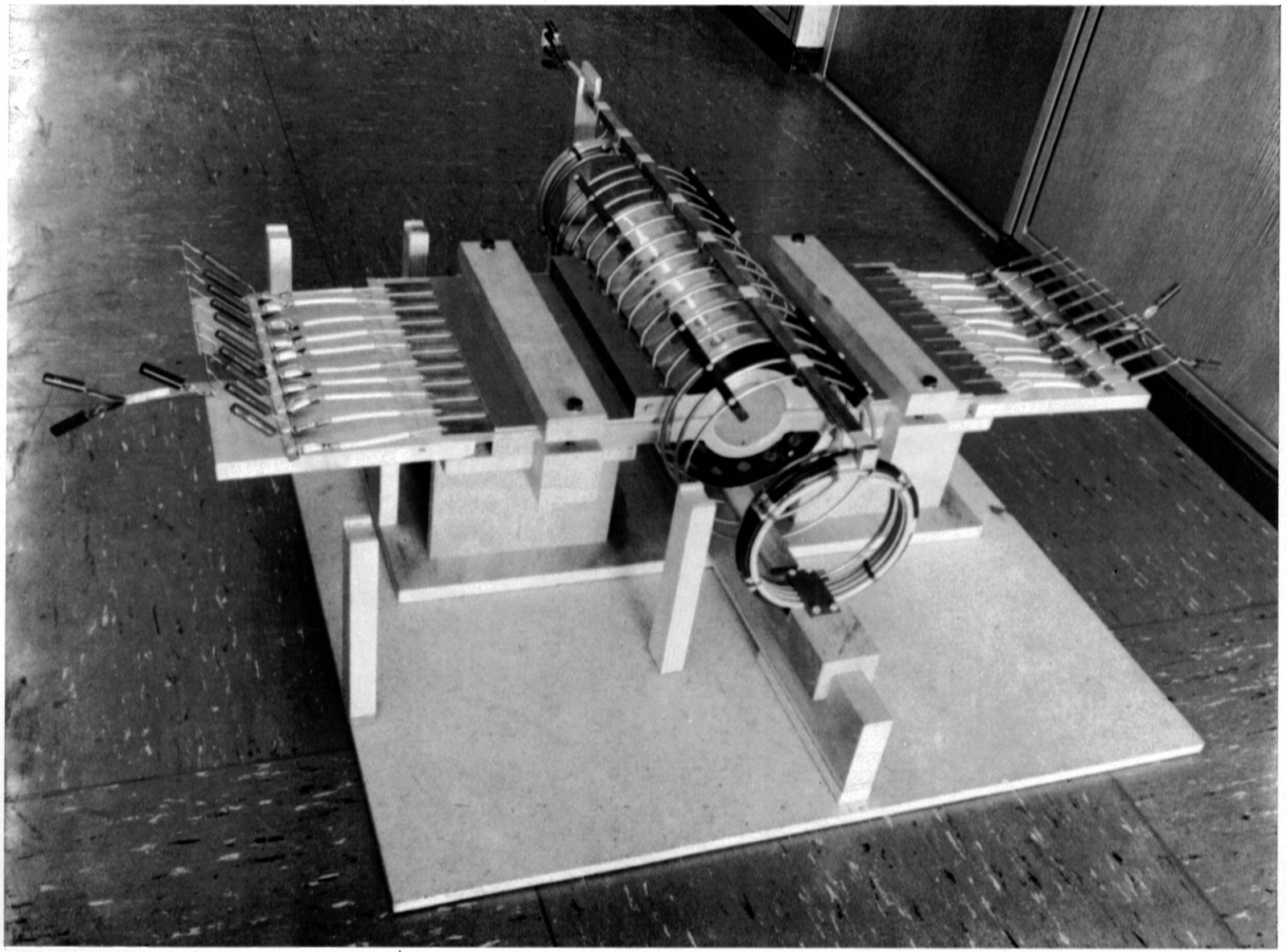

P 029 Turbulence Heating Experiment
Model of main and bias field coils

This work was performed under the terms of the agreement on association between the Institut für Plasmaphysik and Euratom.